JOURNAL OF OPTOELECTRONICS AND ADVANCED MATERIALS Vol. 9, No. 6, June 2007, p. 1803 - 1807

Ultrasonic spectroscopy of welded cryogenic materials

R. ZAGAN, P. PETCULESCU*
"OVIDIUS" University of Constanta, Mamaia Ave. 124, 900527, Constanta, Romania

The purpose of this paper is to analyze the frequency spectrum of the ultrasonic response of a cryogenic material sample using a nondestructive method. The experimental measurements presented here were obtained by the direct contact method using silicon gel as the coupling medium with the pulse-echo technique, with a 5MHz transducer (Nortec). The instrumentation consisted of an IPR-100 signal generator, an A/D-90 converter and SMC-4 step by step motors from Physical Acoustic Corporation, a sampler and a spectral analyzer. The ultrasonic testing of the welded cryogenic material 10TiNiCr180 was made in the base material (point A1) and in the weld (point A3) without being exposed to a thermal treatment (sample B). After that, the material was exposed to the following thermal treatments: first - welding + hardening (sample 2) and the second welding + hardening + annealing treatment (sample 2p). Because Spectral Peak Ratio was known, it was possible to determine the grain size which was compared with the one obtained by the metallographic analysis. It is noticed a decrease of the grain size after the first thermal treatment (46.5 µm), but a small increase after the second thermal treatment (48.7µm), and we identify some resonance numbers of frequencies 1.46MHz, 2.468MHz, 2.719MHz, using ultrasound spectroscopy obtained by Power Spectral Density.

(Received November 14, 2006; accepted April 26, 2007)

Keywords: Ultrasounds, Peak frequency, Power Spectral Density, Spectral Peak Ratio

1. Introduction

Industrial steels applications at low temperatures lead to different studies that tend to increase both the capacity and safety of the equipment in this field. According to the exploitation temperature and utilization conditions, cryogenic materials can be classified as: Al, Cu, Ni, Ti, Li, Mg, etc. non-ferrous alloys; cryogenic irons; Ni steels; Cr-Ni austenitic steels. Out of the many steels specially made for low temperature application, the optimal steel brand is chosen after a detailed study of its utilization and mechanical properties.

Cryogenic steels can be used in aeronautic, food, chemical, petrochemical and transportation industries to manufacture equipments, claddings, and pipes and also to joint them by welding in order to obtain, stock and transport fluids which reach low temperatures while using them. Our scope is to obtain crystalline structures closer to the perfect ones, the control of dislocations density and their displacement, the allying with elements which form substitution solid solutions, the grain sizes increase. The main alloying element in cryogenic steels is Ni because it manifests a strong positive influence on the fragility threshold, 6%Ni lowering the transition temperature at -200°C, the resilience is excellent and the plasticity is high. In many cases, physical, chemical, mechanical and technological properties of metallic materials depend on the applied thermal treatments (re-annealing treatment, annealing treatment, hardening, slackening); for austenitic stainless steels, the applied thermal treatments give a better corrosion resistance.

The welding procedures are the followings:

- Joints preparation has been done in accordance with SR EN 29692:1994 stipulations. This standard refers to manual metal arc and metal protected gas welded joints.
- E19.9.Nb.B.22 electrodes were used as welding materials.
- Welding conditions elaboration has been done by ensuring the geometrical configuration as well as the conditions necessary to obtain physical and mechanical properties and the required welded joint quality. These requirements involve the welding conditions elaboration on scientific bases using analytical relations in order to establish the necessary parameters according to the basic parameters.

A major concern, when welding the austenitic stainless steels, is the susceptibility to cracking. These cracks are primarily due to low-melting liquid phases, which allow boundaries to separate under the thermal and shrinkage stresses during weld solidification and cooling.

Even with the serious cracking concerns, the austenitic stainless steels are generally considered the most weldable stainless steels. For example, the thermal conductivity of austenitic alloys is roughly half that of ferrite steel. Therefore, the weld heat input that is required to achieve the same penetration is reduced. In contrast, the coefficient of thermal expansion of austenite is 30 to 40% greater than that of ferrite, which can result in increases in both distortion and residual stresses, due to welding. The molten weld pool of the austenitic stainless steels is commonly more viscous, or sluggish, than ferrite and martensitic steels. This slows down the metal flow and weldability of welds in austenitic alloys, which may promote lack-of-fusion defects.

2. Experimental set-up

By sampling the ultrasonic response with a correct chosen frequency and then by its digitization, it can be analyzed using the processing technique, obtaining the values of the received signal parameters. Because of the required conditions regarding the limited period of time of the emissed and received signals, one will proceed at the simultaneous analysis of the signals in the time domain and in the frequency domain using the Fourier Transform in the time-frequency domain.

The Fourier transform F(t) in the frequency domain is computed from *f(t)* in the time domain by the direct integration of the relation:

$$F(f)=\int_{-\infty}^{+\infty} f(t)e^{-j2\pi ft}\,dt \tag{1}$$

This type of representation suggests that the analyse of the ultrasonic response is made in a bidimensional space-time-frequency. The idea of using this bidimensional representation is due to the fact that its spectrum is not constant in time but it changes from time to time depending on the evolution of the noise which strongly affects the detection performances. Due to this fact, the analysis of the ultrasonis response spectrum is necessary to be done all the time. In order to process the ultrasonic response using digital systems, the signals must be analyzed and processed in the discrete domain. Therefore, the ultrasonic response is considered to be digitized with one sampling period of the signal in the time domain and with one sampling rate of the signal in the frequency domain. Generally, the frequency bandwidth of the ultrasonic response is limited due to the performances of the receiver transducer. Moreover, a natural limitation of the received signal appears from the propagation medium. Due to these causes, one can consider a maximum (peak) frequency used in the ultrasonic response processing and a maximum banwidth frequency of the receiver transducer.

Generally, a square representation of the signal in the time-frequency domain is given by an energetic representation. This representation can be interpreted as an indicator of the manner the signal energy is distributed in time and also in frequency. The availability of the interpretation of this representation as a density of energy is also given by the manner this representation satisfies other specific properties. Among them is the one which requires that the integration in the time domain to represent the power spectral density (PSD) and in the frequency domain to have the meaning of a momentary power of the signal.

The power spectrum function G(t) is linked with F(t) by the following relation:

$$G(f)=\frac{2}{T}\left|F(t)\right|^{2} \tag{2}$$

The power spectrum density shows the energy distribution in the frequency domain and highlights the main frequency in the signal.

Power spectral density distribution in the time-frequency domain gives a clear image of the concentration mode of the received signal energy but has the disadvantage of an obvious presence of the interference terms (oscilations in the time-frequency plane) making difficult the physical interpretation of this distribution. The solution consists of finding a distribution capable of making an acceptable compromise between the suitable terms of the received signal power and those of the interference.

The experimental measurements presented here were obtained by the direct contact method using silicon gel as the coupling medium with the pulse-echo technique, with a 5MHz transducer (Nortec).The instrumentation consisted of an IPR-100 signal generator, an A/D-90 converter and SMC-4 step by step motors from Physical Acoustic Corporation (Fig. 3).

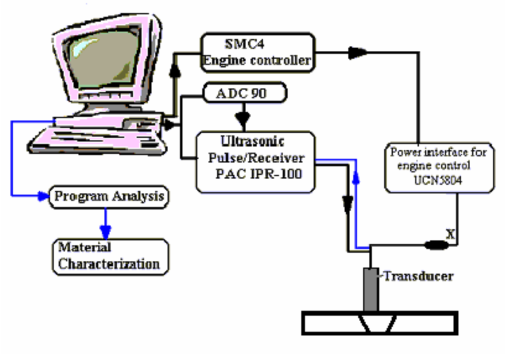

Fig. 1. Experimental set-up.

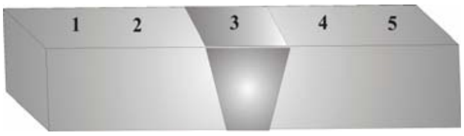

Fig. 2. Sample B.

The signals received from the sample by the 5MHz transducer were sent to an oscilloscope, where their amplitude and velocity was read directly and to the sampler. The signals from the sampler were transmitted to the spectral analyzer where the spectrum of the concerned signal was photographed.

The measurements were performed on the austenitic steel sample 10TiNiCr180 having the following chemical composition in %: C-0.034, Si-0.69, Mn-1.70, Cr-18.55, Ni-9.41, Mo-0.28, Cu-0.35, Ti-0.0018, Nb-0.049, Al-0.068, W-0.085, V-0.061, Co -0.24.

3. Results

The ultrasonic testing of the cryogenic material 10TiNiCr180 was made in the base material (point A1) and in the weld (point A3) without being exposed to a thermal treatment (sample B) (Fig. 2).

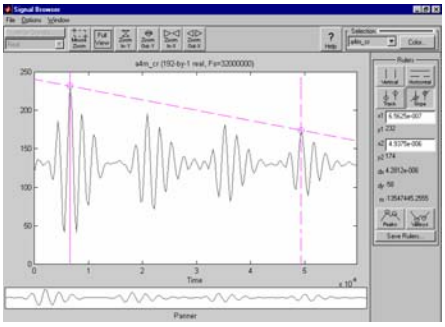

x1 6.5625e-007
y1 232
x2 4.9375e-006
y2 174
dx 4.2812e-006
dy -58
m -13547445.2555

a)

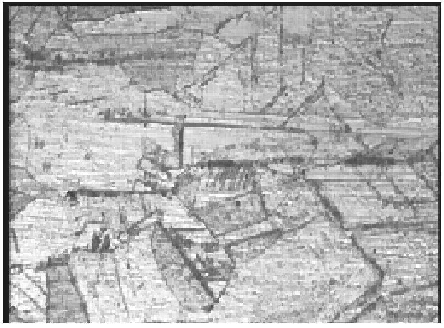

b)

Fig. 3. Ultrasonic echo waveform for sample B (a) and its metallographic structure (b).

The waveform and the metallographic structure of the sample B (without thermal treatment) in the base material (point A1) are shown in Fig. 3. There are shown 4 successive back wall echoes obtained by the contact method and the pulse-echo technique.

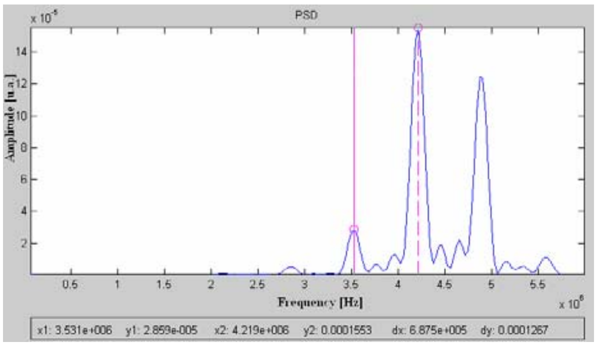

x1: 3.531e+006 y1: 2.859e-005 x2: 4.219e+006 y2: 0.0001553 dx: 6.875e+005 dy: 0.0001267

Fig. 4. The frequency spectrum for sample B.

The frequency spectrum as it is shown in Fig. 4 is given by the following frequencies: 2.83MHZ, 3.53MHz, 4.21 MHz, 4.87 MHz.

After that, the material was exposed to two thermal treatments: welding + hardening (sample 2) and then welding + hardening + annealing treatment (sample 2p). Metallographic tests which emphasize the grains and their changes due to the thermal treatment to which they are submitted were mare for all the three samples. It was noticed the existence of chromium carbide in the base material and in the weld. The frequency spectrum of the ultrasonic response obtained by PSD (Power Spectral Density) shows a prevalent austenitic structure in the base material and in the weld prevails a structure compounded of austenitic + ferrite + Cr carbide.

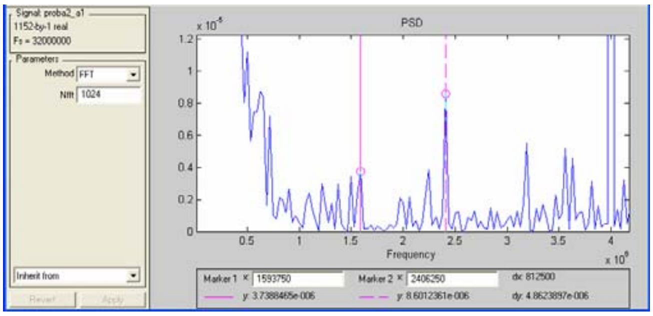

Signal: proba2_a1
1152-by-1 real
Fs = 32000000
Method FFT
Nfft 1024
Marker 1 x 1593750 y: 3.7388465e-006
Marker 2 x 2406250 y: 8.6012361e-006
dx: 812500
dy: 4.8623897e-006

a)

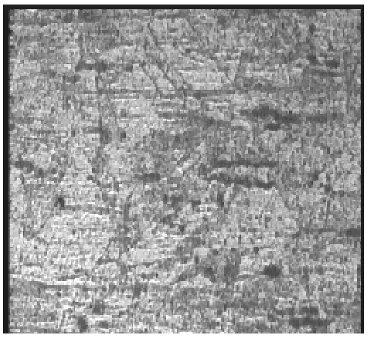

b)

Fig. 5. The frequency spectrum for sample 2 (a) and its metallographic structure (b).

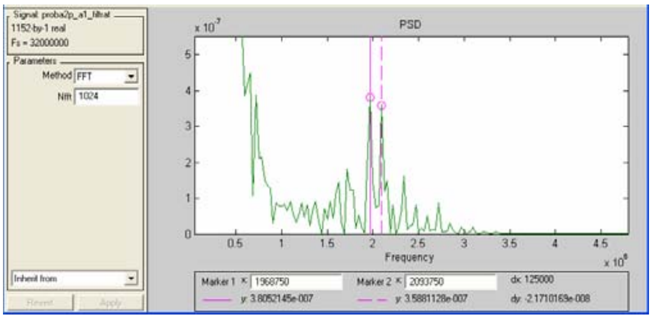

Signal: proba2p_a1_filtrat
1152-by-1 real
Fs = 32000000
Method FFT
Nfft 1024
Marker 1 x 1968750 y: 3.8052145e-007
Marker 2 x 2093750 y: 3.5881128e-007
dx: 125000
dy: -2.1710169e-008

a)

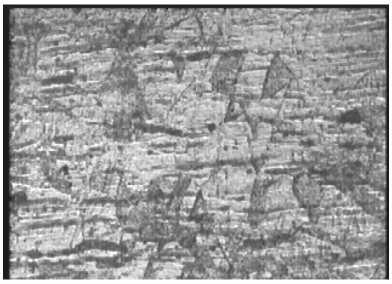

b)

Fig. 6. The frequency spectrum for sample 2p (a) and its metallographic structure (b).

Power spectral density for sample 2 in the base material (point A1) after the thermal treatment of welding +hardening is shown in Fig. 5a and its metallographic structure is shown in Fig. 5b. One can notice here the existence of many important frequencies with significant maxima such as 1.594 MHz, 2.406 MHz, 3.187 MHz, 3.562 MHz, 3.625 MHz.

Then, by applying another thermal treatment of welding + hardening + annealing to the same sample (sample 2p), one obtain a power spectral density showed in Fig. 6a and its metallographic structure (Fig. 6b) in the base material (point A1). After this treatment, the frequency spectrum is compound of the following frequencies: 1.46MHz, 1.625MHz, 1.718MHz, 1.968MHz, 2.093MHz, 2.343MHz, 2.468MHz, 2. 719MHz.

4. Discussion

Because SPR (Spectral Peak Ratio) was known, it was possible to determine the grain size which was compared with the one obtained by the metallographic analysis.

Kumar Anish [1] proved the connection between SPR and the grain size of the austenitic steel microstructure.

Taking into consideration what Kumar [1] proved and determining the correlation coefficient R= 0.9785 in the base material (point A1), one can conclude (see Fig. 7 a and 7b):

- for sample B (without thermal treatment), for SPR = 0.832, the grain size is 62.35 μm;
- for sample 2 (manually welding + hardening), for SPR= 0.814, in the base material, the grain size is 46.5μm, its structure being mostly austenite and in the weld for SPR=0.453, the grain size is 42.38μm, its structure consisting of austenite + ferrite + Cr;
- for sample 2p (manually welding + hardening + annealing) for SPR= 0.807, in the base material the grain size is 48.7μm, its structure being mostly austenite and in the weld for SPR=0.217, the grain size is 38.58 μm, its structure consisting of austenite + ferrite + Cr carbide.

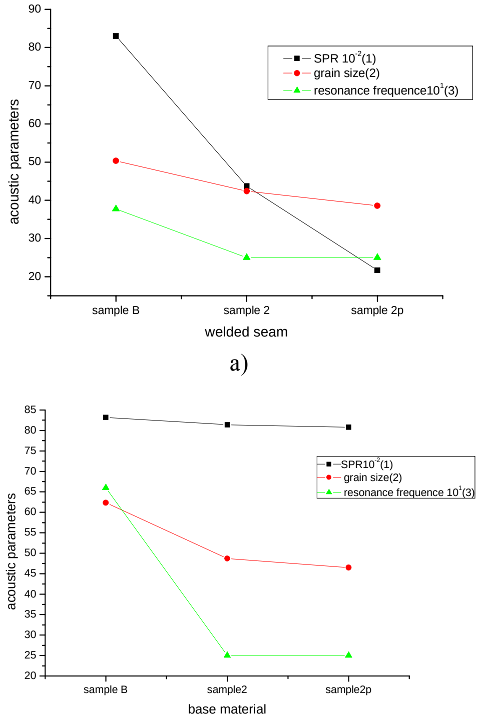

a)

b)

Fig. 7. Variation of acoustic parameters in samples a) welded seam, b) base material.

In the base material structure (point A1), the frequency spectrum distinguishes the existence of the following constituents:

- ➢ sample B (without thermal treatment):
  - ▪ Ferrite (peak frequencies: 2.125 MHz, 2.89 MHz)
  - ▪ austenite (peak frequencies: 3.55 MHz, 4.21 MHz)
- ➢ sample 2 (10TiNiCr180 steel, with thermal treatment: manually welding + hardening)
  - ▪ ferrite (peak frequencies: 3.562 MHz and 3.625MHz);
  - ▪ austenite (peak frequencies: 2.406MHz and 3.187 MHz);
  - ▪ different Cr carbides precipitated at grains limit (peak frequency:1.594 MHz);
- ➢ sample 2p (10TiNiCr180 steel, with thermal treatment manually welding + hardening + annealing):
  - ▪ ferrite (peak frequencies:1.625MHz, 1.718MHz and 2.343 MHz);
  - ▪ austenite (peak frequencies: 1.968 MHz, 2.093MHz),
  - ▪ different chromium carbides precipitated at the grains limit (peak frequencies: 1.46MHz, 2.468 MHz, 2.719MHz).

The classification of frequencies depending on their content in austenite, ferrite and Cr carbide was performed after analyzing the spectrogram amplitudes from PSD in correlation with the bright intensity on the metallographic images [12].

5. Conclusions

The structure of the base material (sample B) is composed of an austenite polyhedral crystal with many twin strips + ferrite. At the microscope, the austenite has a bright color (high bright intensity, see the high amplitude frequencies of 3.55 MHz and 4,21Mhz).

The grain sizes are within the size limits 5-6 according to standard SR ISO 643-1993. The same values for the grain size were obtained by calculating SPR.

For quench hot treated sample2, the base material structure is also composed of austenite polyhedral crystals but with less chromium carbides precipitated at grain limit (see the frequency 1.594 MHz).

It is noticed a decrease of the grain size after the first thermal treatment S (46.5 μm) but a small increase after the second one (48.7 μm).

Applying of the annealing treatment leads to the obtaining of the same polygonal austenite structure but it is noticed an increase of the quantity of Cr carbide also seen from the number of frequencies (1.46 MHz, 2.468 MHz, 2.719 MHz). The presence of a quantity of ferrite in the structure is noticed in all the samples (see the metallographic images and the number of frequencies).

Ultrasonic response have been filtrated and sampled being analyzed in flame spectra using Power Spectral Density (PSD). The obtained flame spectra mark out the occurrence of three structural constituents (austenite, ferrite and chromium carbide) in the base material that has been also confirmed by metallographic analysis.

Material grain size has been determined taking into consideration the connection between Spectral Peak Ratio (SPR) and the grain size microstructure (the metallographic image).

References

[1] A. Kumar, T. Jayakumar, R. Baldev, Philosophical Magazine A, **80**(11), 2469-2487 (2000).

[2] A. Kumar, T Jayakumar, P. Palanichamy, Baldev Raj, Scripta Materialia **40**(3), 333 (1999).

[3] P. Petculescu, R. Ciocan, V. Bokas, Investigation of the austenitic structures by ultrasonic spectral analysis, 7 th ECNDT Copenhaga, 1998 and in Journal of Nondestructive Testing and Ultrasonic **3**(11), (1998).

[4] R. Zăgan, P. Petculescu, I. Lungu, Gh. Mihăieşi, Comparative study A – scan and wavelets analysis through ultrasonic signals, MEET 2002 First International Congress on Mechanical and Electrical Engineering and Technology and MARIND 2002, Technical University of Varna, 07 – 11 october 2002, Varna, Bulgaria, vol.1 ISBN 954-20-0211-4, pp. 229 – 234, (2002).

[5] J. Krautkramer, Ultrasonic testing of materials, Second ed. Springer-Verlag, NewYork (1977).

[6] L. Cohen, Time-Frequency Distributions: A Review, Proc. IEEE, pp. 941-981 (1989).

[7] Signal Processing User’s Guide, Mathworks, (1996).

[8] A. Abbate, J. Koay, J. Frankel, S. C. Schoeder, Signal detection and noise suppression using a wavelet transform signal processor: application to ultrasonic flaw detection, IEEE Trans. Ultrason., Ferroelect., and Freq. Contr. **44**(1), 14-25 (1997).

[9] P. M. Gammell, Analogue implementation of analytic signal processing for pulse-echo systems, Ultrasonics, pp. 279-283 (1981).

[10] P. Petculescu, R. Ciocan, D. Ciobanu, Automated system and automated method by ultrasonic investigation, patent no. 118612B, RO.

[11] L. Lin, X. M. Li, J. S. Zhang, Nondestructive differentiation of three transformation products in low alloy steel using two ultrasonic methods, Material Evaluation, pp. 512-516 (2003).

[12] A. Briggs, Acoustic Microscopy, Clarendon Press, Oxford, 1992.

---

*Corresponding author: petculescu@univ-ovidius.ro